SERVO TRACKING OF TARGETS AT SEA

ANIS AHMED[*,**], MIECZYSŁAW A. BRDYŚ[*]

[*] Department of Electronic, Electrical and Computer Engineering
School of Engineering, University of Birmingham
Birmingham B15 2TT, UK
e-mail: m.brdys@bham.ac.uk

[**] Pilkington Glass, Pilkington Cowley Hill
St. Helens, WA10 2RZ, UK
e-mail: Anis.Ahmed@pilkington.com

This paper details a proposal for the position control system of a two-axis ship-mounted tracker. Aspects of the non-linear dynamics governing Line-Of-Sight (LOS) errors between the tracker and the target are presented. It is shown that the regulation of LOS errors can be achieved by introducing a feed-forward term based on the target's velocity. This velocity is not measurable, and an estimator is required. Given that the tracking problem is non-linear, the classical separation principle does not hold, and cascading the estimator and regulator together may not lead to an optimal position control system. The 'LQAdaptive' system proposed here aims therefore to improve conformity to the separation principle. Simulation trials show that tracking is improved under the LQAdaptive system in comparison to a simple estimator-regulator structure.

Keywords: target tracking, tracker, Kalman Filter, adaptive control

1. Introduction

The tracker is a ship-mounted device that is used to follow the path of airborne targets. It is composed of two controllable axes: a training axis, which is always perpendicular to the ship deck, and an elevation axis, which always lies in the plane of the ship deck. The aim of the control system is to drive the tracker axes so that the bore-sight is looking directly at the target, which requires regulation of the angular position errors between the bore-sight and the target Line-Of-Sight (LOS). As shown in Fig. 1, the angular errors are defined by introducing an r-e-d coordinate frame such that the r-axis is always coincident with the tracker sightline, the e-axis is always parallel to the ship deck, and the d-axis points seawards. This allows two errors, namely the pitch and yaw errors, to be defined. Radar and electro-optic sensors provide measurements of these errors. The range of the target from the tracker is also measured.

Feedback is also available of the roll, pitch and yaw angular velocities of the bore-sight about the r, e and d axes, respectively. These velocities are measured by gyros mounted on the bore-sight.

The dynamics of the pitch and yaw errors are related to the angular velocities of the tracker in the constructed r-e-d frame. A position controller can therefore be designed that receives the available sensor data and then controls the tracker's pitch velocity ω_e and yaw velocity ω_d in order to reduce the pitch and yaw errors. Details of the error dynamics are given in Section 2.

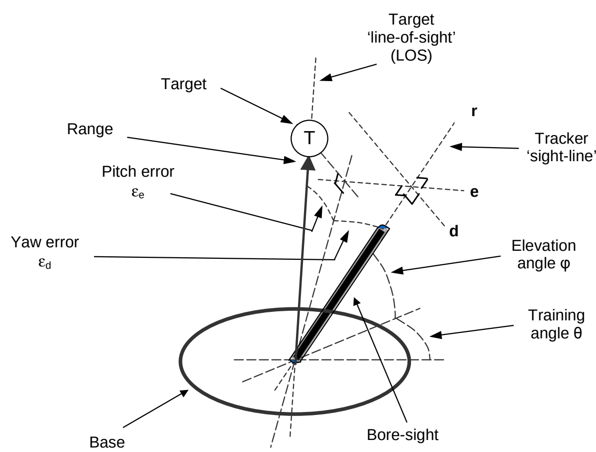

Fig. 1. Tracker angles.

The pitch velocity set point can be actuated directly by the elevation axis, since the pitch axis and elevation axis always coincide, but this is not always the case for the yaw and training axes. Figure 2 shows how the position of the yaw axis is dependent on the elevation angle φ. As the bore-sight elevation angle tends towards 90^o, an increasing large rate $\dot{\theta}$ is required by the training axis in order to generate the desired angular velocity ω_d in the

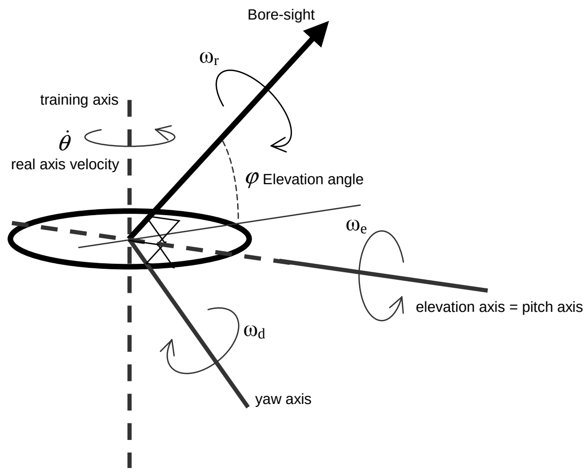

Fig. 2. Tracker velocities.

yaw axis. In reality, the control system would only be able to operate safely up to elevation angles of around 70^o.

The actuation of the tracker axes must account for the dynamics of the physical hardware, as well as disturbances such as stiction, wind torques and ship motion. For this purpose, a separate velocity controller is used that receives the angular velocity set points from the position controller and then implements them. Work has already been carried out on the design of the velocity controller, with the use, for example, of fuzzy logic gain scheduling to handle the non-linear friction effects. For the purposes of position controller design, in this paper it will be assumed that the velocity controller achieves perfect and instant actuation of any set points it receives. Further details of velocity controller design can be found in (Brdyś and Littler, 2002). Figure 3 gives the overall structure of the tracker control system.

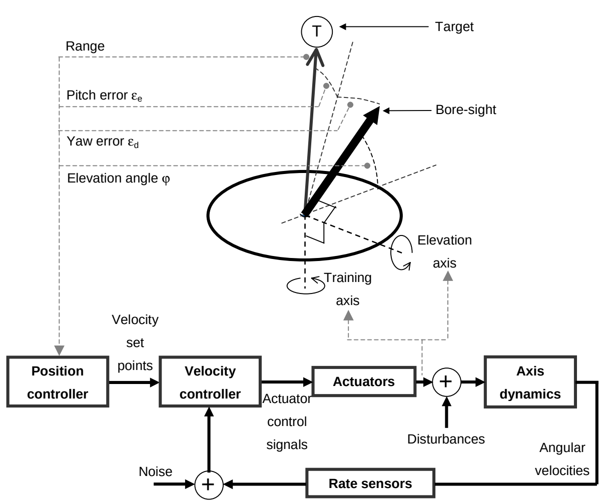

Fig. 3. Overall structure of the tracker control system.

In addition to the tracker angular velocities, the pitch and yaw error dynamics are also related to the target angular velocities. The analysis in Section 3.1 shows that the regulation of the position errors is achieved if the regulator is based on both the feedback of the errors and feedforward compensation of the target velocities.

However, the target's angular velocities cannot be measured directly, and thus estimates of these are required. A common solution to the estimation problem is to use a Kalman filter. The filter is based on a dynamic model that relates the known range and error data to the required velocities, with uncertainties in the dynamics being represented by white noise. The details of the model are presented in Section 2.

The simplest approach to designing the position controller would be to cascade the estimator and the regulator together. From a practical viewpoint, this would be the ideal solution since both the required Kalman filter and the regulator are already commercially available as individual components that independently work well. The development time would therefore be minimal. The cascaded position controller can be seen in Fig. 4.

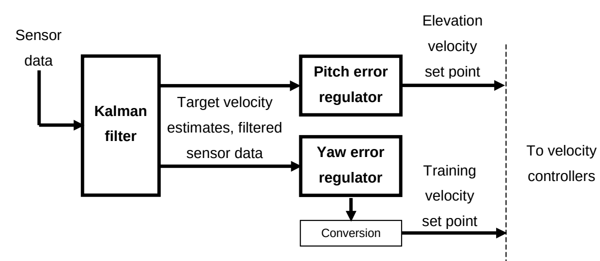

Fig. 4. Simple cascaded position controller.

During operation, the estimator would filter real input sensor data, and also generate estimates of immeasurable states. The filtered sensor data and the estimates would then be treated as true input data by the regulator — a case of the 'certainty equivalence principle'. Since the estimator would provide the required data, and the regulator would be tuned to achieve the required tracking characteristics, it could be assumed that the cascaded system would be the overall optimal position control system.

Unfortunately, this is unlikely to be the case. The optimality of the overall system assumes that the 'linear separation principle' applies (Kwakernaak and Sivan, 1972), which states that if the estimator is a linear mean-square-optimal filter, and the regulator is designed using optimal linear state feedback techniques, then the cascaded estimator-regulator does indeed result in the optimal closed-loop control system. In this problem, the dynamics are non-linear, and the regulator is designed by the inspection of these dynamics. Thus, the 'linear separation principle' is unlikely to hold, and the performance of the closed-loop system is likely to be sub-optimal.

In Section 3.2, a position control system is proposed that aims to integrate the filter based on the non-linear dynamics with the regulator designed by inspection. The guiding principle behind the development is to conform as closely as possible to the separation principle. This is achieved by introducing local linearization and filtering based on standard techniques, such that the components are at least locally linear-optimal. Under the assumption of perfect velocity control, cascading these independently designed components together leads to a closed loop control system with improved tracking performance compared to the simple estimator-regulator structure. Details of the proposal are given Section 4, and simulation data is provided in Section 5.

2. Kinematic Model

The differential equations governing Line-Of-Sight (LOS) dynamics are already well established and used, e.g., in guidance systems for homing missiles. The LOS dynamics model can also form the basis of the control system for the ship-based tracker.

A full derivation of the LOS model can be found in (Ekstrand, 2001), but the key ideas are as follows: The r-e-d coordinate frame is based on the tracker, with the r-axis representing the bore-sight. A second coordinate frame labelled r'-e'-d' is introduced based on the target LOS, where the r'-axis lies on the LOS itself. Similar to the e-axis, the e'-axis is defined as being parallel to the ship deck.

The tracker must move so that the r-e-d frame coincides with the r'-e'-d' frame. This is achieved by a sequence of two rotations — first, a yaw angle ε_d about the d-axis, which brings the e-axis in line with the e'-axis and, secondly, a pitch angle ε_e about the e-axis in its new position. This sequence brings the r-axis into line with the r'-axis, which in reality means the bore-sight is now on the LOS. Only two rotations are required since the e-axis and e'-axis always lie in the same plane. Both the tracker r-e-d and target r'-e'-d' frames will have inertial angular velocities, which can be expressed in their respective coordinate frames. The tracker velocity is

$$\bar{\omega} = \begin{bmatrix} \omega_r \\ \omega_e \\ \omega_d \end{bmatrix},$$

while the target velocity is

$$\bar{\omega}' = \begin{bmatrix} \omega'_r \\ \omega'_e \\ \omega'_d \end{bmatrix}.$$

The following relation holds true:

$$\bar{\omega}' - M\bar{\omega} = \begin{bmatrix} -\dot{\varepsilon}_d \sin\varepsilon_e \\ \dot{\varepsilon}_e \\ \dot{\varepsilon}_d \cos\varepsilon_e \end{bmatrix}, \tag{1}$$

where

$$M = \begin{bmatrix} \cos\varepsilon_e\cos\varepsilon_d & \cos\varepsilon_e\sin\varepsilon_d & -\sin\varepsilon_e \\ -\sin\varepsilon_d & \cos\varepsilon_d & 0 \\ \sin\varepsilon_e\cos\varepsilon_d & \sin\varepsilon_e\sin\varepsilon_d & \cos\varepsilon_e \end{bmatrix}$$

is the coordinate transformation matrix to express the tracker rate $\bar{\omega}$ in terms of the LOS frame r'-e'-d'.

By substituting the matrix M and the component vectors of $\bar{\omega}$ and $\bar{\omega}'$ into (1), and simplifying with the small angle approximations $\sin\theta \approx \theta$ and $\cos\theta \approx 1$, the following relationships can be derived:

$$\begin{aligned} \dot{\varepsilon}_e &= \omega'_e - \omega_e + \omega_r\varepsilon_d, \\ \dot{\varepsilon}_d &= \omega'_d - \omega_d - \omega_r\varepsilon_e. \end{aligned} \tag{2}$$

The equations in (2) show that the pitch and yaw errors are coupled via the tracker roll rate ω_r. Although in some applications the roll rate may be discounted, in the case of the tracker the roll rate is significant because the rotation about the training axis leads to both ω_d and ω_r velocity components.

The equations also show that the errors depend on the target pitch rate ω'_e and yaw rate ω'_d, neither of which is controllable nor measurable. However, a model of these rates was developed (Ekstrand, 2001) based on the target range and acceleration.

In the LOS r'-e'-d' frame, the measurable acceleration of the tracker is denoted as

$$\bar{a}_I = \begin{bmatrix} a_{Ir'} \\ a_{Ie'} \\ a_{Id'} \end{bmatrix},$$

and the immeasurable acceleration of the target is denoted as

$$\bar{a}_T = \begin{bmatrix} a_{Tr'} \\ a_{Te'} \\ a_{Td'} \end{bmatrix}.$$

It is also known that the target is a distance R along the LOS, such that its coordinate position in the LOS frame can always be described as

$$\bar{r} = \begin{bmatrix} R \\ 0 \\ 0 \end{bmatrix}.$$

Since the target is moving, the LOS frame is rotating, and the rotation matrix based on the target angular velocity can be stated as

$$\tilde{\omega}' = \begin{bmatrix} 0 & -\omega'_d & \omega'_e \\ \omega'_d & 0 & -\omega'_r \\ -\omega'_e & \omega'_r & 0 \end{bmatrix}.$$

From rotational mechanics, the following relation holds true:

$$\bar{a}_T = \bar{a}_I + \ddot{\bar{r}} + \dot{\tilde{\omega}}'\bar{r} + 2\tilde{\omega}'\dot{\bar{r}} + \tilde{\omega}'\tilde{\omega}'\bar{r}. \tag{3}$$

Substituting the vector components into (3) and rearranging it gives the following:

$$\dot{\omega}'_e = -2\frac{\dot{R}}{R}\omega'_e - \frac{a_{Td'} - a_{Id'}}{R} + \omega'_r\omega'_d, \tag{4}$$

$$\dot{\omega}'_d = -2\frac{\dot{R}}{R}\omega'_d - \frac{a_{Te'} - a_{Ie'}}{R} - \omega'_r\omega'_e, \tag{5}$$

$$\ddot{R} = \left(\omega_d'^{\,2} + \omega_e'^{\,2}\right) R + a_{Tr'}. \tag{6}$$

Finally, the well-known Singer acceleration model (Singer, 1970) can be used for modelling the unknown target accelerations. For the r'-axis, it is

$$\dot{a}_{Tr'} = -\frac{1}{\tau}a_{Tr'} + w_{aTr'}, \tag{7}$$

where τ stands for the target manoeuvre time constant which is set to represent the expected manoeuvring of the target, and $w_{aTr'}$ is the white noise representing uncertainty in the knowledge of the acceleration value. This model was recently generalised for mulltiple target tracking purposes (Yang, 2002).

Thus, among Eqns. (2) and (4)–(6) and the acceleration models, a model is available for the pitch and yaw error dynamics, as well as the target angular velocities. This model now forms the basis for the control system design.

3. Controller Structure

3.1. Basic Regulator. As has already been stated, the tracker has to regulate the pitch and yaw errors to zero so that it is looking directly at the target. The equations in (2) can be used to design the regulator, and our analysis will focus on the pitch axis since the yaw axis follows similar lines. The pitch error dynamics are stated again as

$$\dot{\varepsilon}_e = \omega'_e - (\omega_e + d_{\omega e}) + \omega_r\varepsilon_d, \tag{8}$$

where ε_e is the pitch error, ω'_e denotes the target pitch rate, ω_e means the controlled tracker pitch rate, $d_{\omega e}$ signifies the error in tracker pitch rate actuation, ω_r is the tracker roll rate, and ε_d stands for the yaw error.

Looking at Eqn. (8), it is clear that compensation is required of the target rate ω'_e and the coupling term $\omega_r\varepsilon_d$. It is the compensation of ω'_e that gives rise to the need for an estimator. The feedback of the filtered position error is also required in order to drive the error in the closed loop system to zero.

The regulator can be formulated as

$$\omega_e = (\omega'_e + d_{\omega' e}) + \omega_r(\varepsilon_d + d_{\varepsilon d}) + k_p(\varepsilon_e + d_{\varepsilon e}) + k_i \int (\varepsilon_e + d_{\varepsilon e})\,\mathrm{d}t, \tag{9}$$

where $d_{\omega' e}, d_{\varepsilon d}, d_{\varepsilon e}$ stand for the errors in the estimates of the target pitch rate, yaw error and pitch error, respectively, and k_p, k_i are proportional and integral feedback gains.

Substituting (9) into (8) leads to the following closed loop dynamics:

$$\ddot{\varepsilon}_e + k_p\dot{\varepsilon}_e + k_i\varepsilon_e = -\dot{d}_{\omega' e} - \dot{\omega}_r d_{\varepsilon d} - \omega_r\dot{d}_{\varepsilon d} - k_p\dot{d}_{\varepsilon e} - k_i d_{\varepsilon e} - \dot{d}_{\omega e}. \tag{10}$$

The analysis of the terms on the right-hand-side of (10) reveals that any constant actuation error is rejected. Constant biasing of the estimates is partially rejected, with two unwanted error drivers, $\dot{\omega}_r d_{\varepsilon d}$ and $k_i d_{\varepsilon e}$, remaining. If the first product term is not significantly large and the integral gain not set too high, then the error dynamics are

$$\ddot{\varepsilon}_e + k_p\dot{\varepsilon}_e + k_i\varepsilon_e = 0. \tag{11}$$

Thus the pitch error will asymptotically converge to zero with the rate determined by the tuned gains k_p and k_i, and error convergence is independent of the actual tracking profile.

3.2. Proposed Structure. With the regulator in (9), the data input requirements are an estimate of the immeasurable target pitch rate, and filtered pitch and yaw errors in order to suppress the effect of measurement noise. An extended continuous Kalman filter can be developed based on the non-linear kinematics model presented in Section 2 that can receive the raw radar and sensor data, and generate estimates of the required data inputs. Cascading the filter and the regulator together would form the simplest structure for the closed loop system.

However, as has already been discussed, the performance of this system is likely to be sub-optimal since there is no 'separation principle' for non-linear problems, and open-loop performance of the estimator and regulator is unlikely to be maintained in the closed loop.

In order to get better conformity to the separation principle, a series of modifications can be made to the estimator-regulator structure.

Local Filtering
Separation assumes that the regulator is based on Linear-Quadratic (LQ) optimal full state feedback design, and full feedback implies that the regulator and estimator are working in the same state-space. It can be seen that, in this case, the regulator is only using limited information on the target velocities and position errors, whereas the extended continuous Kalman filter is based on the full LOS model that also includes range and acceleration states. The regulator is as such designed on a subset of the full state-space.

Applying full state feedback design to the complete set of states in the LOS model would be unwise, since many of the states, such as the target range, are uncontrollable, and the design procedure would be unsolvable. Thus, in order to be able to apply optimal state feedback design, a local Kalman filter is inserted between the main Kalman filter and the regulator. The function of this local filter is to ensure that the regulator is directly connected to an estimator working on the same state space. The local filter treats estimates of the position errors from the main filter as sensor inputs. Target velocity estimates are treated as measured disturbance signals since they are uncontrollable. The local filter then produces estimates of the position errors and of the integral of the errors for use in the feedback part of the regulator.

Linearization
An extended continuous Kalman filter works by producing continuous estimates based on the known non-linear dynamics, but updates at discrete time points by linearizing the dynamics at that instant and basing the update gain on the local linear dynamics. Although not proven to be optimal in the least-square-error sense, it is possibly the best application of the known optimal filters to non-linear problems.

Since optimal state-space feedback design of regulators applies only to linear dynamics, the opportunity arises to make further use of local linear dynamics already calculated in the filter. A regulator such as (9) would require the tuning of the k_p and k_i gains with respect to some expected scenario of target profiles and disturbances, but redesigning the regulator at each point of linearization would produce a more versatile controller that could react to the individual profiles and disturbances at each instant. Furthermore, the regulator would be based on LQ optimal linear design, which improves the conformity of the overall system to the separation principle.

Linearization is carried out by the Taylor series expansion of the dynamics about the operating point at that instant. This leads to a constant term that depends on the operating point. A compensation signal is required in the regulator to cancel the effect of the constant term in order to leave a standard linear dynamic system. LQ optimal state-space feedback design can then be applied to this linear system. Hence, the overall regulator is still composed of a feed-forward compensation term and feedback based on the position errors.

Given that the regulator is adapted to the local linear dynamics, and the design is based on LQ optimal control, the proposed new control system is labelled the 'LQAdaptive' structure. A diagrammatic representation of the simple estimator-regulator structure can be seen in Fig. 5, while the LQAdaptive structure is given in Fig. 6.

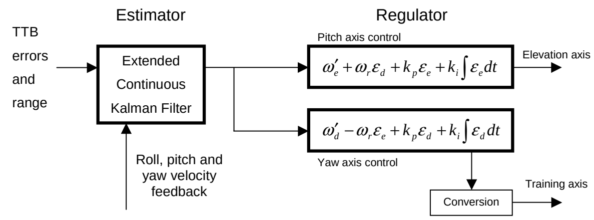

Fig. 5. Simple estimator-regulator structure.

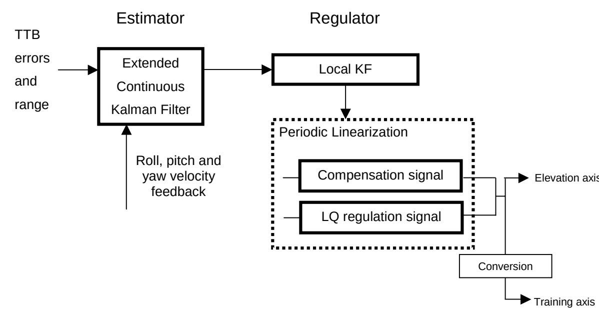

Fig. 6. Proposed LQAdaptive structure.

4. LQAdaptive Formulation

4.1. LOS Model. The component parts of the structure can now be presented. Parts of the LOS model have already been presented in Section 2 but, for clarity, the following is the complete model:

- range equation:
$$\ddot{R} = \left(\omega_d'^{\,2} + \omega_e'^{\,2}\right) R + a_{Tr'}, \tag{12}$$
- disturbance input to range equation:
$$\dot{a}_{Tr'} = -\tfrac{1}{\tau} a_{Tr'} + w_{aTr'}, \tag{13}$$
- pitch error:
$$\dot{\varepsilon}_e = \omega_e' - \omega_e + \omega_r \varepsilon_d, \tag{14}$$
- target pitch angular velocity:
$$\dot{\omega}_e' = -2\frac{\dot{R}}{R}\omega_e' - \frac{a_{Td'} - a_{Id'}}{R} + \omega_r'\omega_d', \tag{15}$$
- disturbance input into pitch angular rate:
$$\dot{a}_{Te'} = -\tfrac{1}{\tau} a_{Te'} - \omega_r' a_{Td'} + w_{aTe'}, \tag{16}$$
- yaw error:
$$\dot{\varepsilon}_d = \omega_d' - \omega_d - \omega_r \varepsilon_e, \tag{17}$$

- target yaw angular velocity:
$$\dot{\omega}'_d = -2\frac{\dot{R}}{R}\omega'_d - \frac{a_{Te'} - a_{Ie'}}{R} - \omega'_r\omega'_e, \tag{18}$$
- disturbance input into yaw angular rate:
$$\dot{a}_{Td'} = -\tfrac{1}{\tau}a_{Td'} - \omega'_r a_{Te'} + w_{aTd'}. \tag{19}$$

4.2. Extended Kalman filter. The extended continuous Kalman filter algorithm with discrete measurements (Borrie, 1992; Jaźwiński, 1970) is a cycle consisting of a continuous estimation phase followed by a discrete update phase. A general non-linear system is given as

$$\begin{aligned} \dot{x}_t &= A\left(x_t, u_t, t\right) + \Gamma w_t, \\ y_k &= H\left(x_k, k\right) + v_k, \end{aligned} \tag{20}$$

where x_t is the continuous state, u_t is the continuous input, y_k are discrete measurements, A, H are respectively non-linear system and measurement functions, Γ denotes the noise matrix, and w_t, v_k represent non-correlated additive white Gaussian noise with a positive semi-definite covariance matrix Q and a positive definite covariance matrix R, respectively.

The estimates $\hat{x}_t$ are generated using

$$\dot{\hat{x}}_t = A\left(\hat{x}_t, u_t, t\right). \tag{21}$$

The associated covariance matrix P is calculated using the equation

$$\dot{P}_{t|k-1} = A_{k|k-1}P_{t|k-1} + P_{t|k-1}A^T_{k|k-1} + \Gamma Q \Gamma^T, \tag{22}$$

where $P_{k-1|k-1}$ is the initial condition in (22).

The matrices $A_{k|k-1}$ and H_k are first-order linearized approximations of the functions A and H at the previous update, and are calculated as

$$A_{k|k-1} = \left[\frac{\partial A}{\partial x}\right]_{x=\hat{x}_{k|k-1}}, \quad H_k = \left[\frac{\partial H}{\partial x}\right]_{x=\hat{x}_{k|k-1}}. \tag{23}$$

After calculating the linearized approximations, updates at the measurement instants are calculated in three steps. First, the Kalman gain K is calculated,

$$K_k = P_{k|k-1}H^T_k\left(H_k P_{k|k-1} H^T_k + R\right)^{-1}. \tag{24}$$

Next, state updates occur based on the new measurements y_k:

$$\hat{x}_{k|k} = \hat{x}_{k|k-1} + K_k\left(y_k - H\left(\hat{x}_{k|k-1}, k\right)\right). \tag{25}$$

Finally, the covariance matrix P is updated:

$$P_{k|k} = P_{k|k-1} - K_k H_k P_{k|k-1}. \tag{26}$$

The algorithm embodied by (21)–(26) can be applied to the LOS model in (12)–(19), with the differential equations representing the non-linear functions A. The measurement function H is simply a matrix that selects the pitch error, yaw error and range from the state vector, since these are the states that are directly measured. The linearization of H is therefore unnecessary in this case. The covariance matrix Q is set to represent the level of uncertainty in the acceleration models, while the covariance matrix R represents the sensor noise in the three measurements. The control inputs are the tracker pitch and yaw angular velocities ω_e and ω_d. Data such as the tracker roll rate ω_r and accelerations are treated as measured inputs, but sensor noise associated with these measurements has not been represented in the model.

4.3. Local Filter. The smaller local Kalman filter is based on the following dynamics:

$$\begin{aligned} \dot{\varepsilon}_e &= \omega'_e + \omega_r\varepsilon_d - \omega_e + w_{\omega' e}, \\ \dot{\varepsilon}_d &= \omega'_d - \omega_r\varepsilon_e - \omega_d + w_{\omega' d}, \\ \dot{x}_3 &= \varepsilon_e, \\ \dot{x}_4 &= \varepsilon_d. \end{aligned} \tag{27}$$

For this filter, the four differential equations represent the set of non-linear functions A. H is a matrix that selects the pitch and yaw errors from the state vector since these are read as ‘measurements’ from the main filter. The expected level of ‘noise’ on these measurements is set in the covariance matrix R. The independent white Gaussian noise terms $w_{\omega' e}$ and $w_{\omega' d}$ represent uncertainty in the measured disturbance signals ω'_e and ω'_d, respectively, and have a covariance matrix Q. Control inputs are the tracker pitch and yaw angular velocities ω_e and ω_d as expected.

The two state variables x_3 and x_4 are used to provide estimates of the integral of the position errors. This is identical to integrating the output estimates of ε_e and ε_d individually. However, if the integrals are calculated separately outside the filter, then the tuning of the integral gains is required when designing the regulator. By allowing the integral state variables to appear in the linearized dynamics, the LQ optimal regulator design can solve gains for these terms in a single overall problem.

4.4. Linearization. The linearized dynamics are produced by the Taylor series expansion of the known dynamics around the current operating point (x_0, u_0). The dynamics can be stated in general again as

$$\dot{x} = A\left(x, u, t\right). \tag{28}$$

The local dynamics about the operating point can then be approximated by

$$\begin{aligned} \dot{(x + \Delta x)} \; = \; & A\left(x_0, u_0\right) \\ & + \left.\frac{\partial A}{\partial x}\right|_{x_0,u_0}\Delta x + \left.\frac{\partial A}{\partial u}\right|_{x_0,u_0}\Delta u + \text{h.o.t.}, \end{aligned} \tag{29}$$

where $\Delta x = x - x_0$ and $\Delta u = u - u_0$ represent small departures from the given operating point, and h.o.t. stands for higher-order-terms that can be considered insignificant.

Let the matrices of partial derivatives be denoted as

$$A_0 = \left.\frac{\partial A}{\partial x}\right|_{x_0,u_0} \text{ and } B_0 = \left.\frac{\partial A}{\partial u}\right|_{x_0,u_0}. \tag{30}$$

Then the equation in (29) can be rearranged to give

$$\dot{x} \approx A(x_0, u_0) - A_0 x_0 - B_0 u_0 + A_0 x + B_0 u. \tag{31}$$

The first three terms on the right-hand side of (31) form a constant term that has arisen due to linearizing around the particular operating point (x_0, u_0). A compensation term $\tilde{u}$ can be generated, where

$$\tilde{u} = B_0^{-1}\left(A_0 x_0 + B_0 u_0 - A(x_0, u_0)\right). \tag{32}$$

Substituting (32) into (31) leaves a standard linear dynamic system

$$\dot{x} = A_0 x + B_0 \bar{u}, \tag{33}$$

where $\bar{u}$ is designed to control this local approximation.

The process of linearizing and generating compensation signals must be carried out frequently, since the approximation is only valid over a short period of time, and becomes invalid as the true state evolves.

4.5. Feed-Forward Compensation. In the dynamics in (27), the state vector is

$$x = \begin{bmatrix} \varepsilon_e \\ \varepsilon_d \\ x_3 \\ x_4 \end{bmatrix}$$

and the input vector is

$$u = \begin{bmatrix} \omega_d \\ \omega_e \end{bmatrix}.$$

Applying the above process to the dynamics results in

$$A_0 = \begin{bmatrix} 0 & \omega_r & 0 & 0 \\ -\omega_r & 0 & 0 & 0 \\ 1 & 0 & 0 & 0 \\ 0 & 1 & 0 & 0 \end{bmatrix}, \tag{34a}$$

$$B_0 = \begin{bmatrix} 0 & -1 \\ -1 & 0 \\ 0 & 0 \\ 0 & 0 \end{bmatrix}. \tag{34b}$$

Since B_0 has a full rank, its inverse exists, so the feed-forward compensation signal $\tilde{u}$ can be calculated at every point of linearization. Denoting terms at the operating point with a subscript 0, the compensation in (32) can be calculated as

$$\begin{aligned}\tilde{u} = {} & \begin{bmatrix} 0 & -1 & 0 & 0 \\ -1 & 0 & 0 & 0 \end{bmatrix} \\ & \times \left(\begin{bmatrix} 0 & \omega_{r0} & 0 & 0 \\ -\omega_{r0} & 0 & 0 & 0 \\ 1 & 0 & 0 & 0 \\ 0 & 1 & 0 & 0 \end{bmatrix} \begin{bmatrix} \varepsilon_{e0} \\ \varepsilon_{d0} \\ x_{30} \\ x_{40} \end{bmatrix} \right. \\ & + \begin{bmatrix} 0 & -1 \\ -1 & 0 \\ 0 & 0 \\ 0 & 0 \end{bmatrix} \begin{bmatrix} \omega_{d0} \\ \omega_{e0} \end{bmatrix} \\ & \left. - \begin{pmatrix} \omega'_{e0} + \omega_{r0}\varepsilon_{d0} - \omega_{e0} \\ \omega'_{d0} - \omega_{r0}\varepsilon_{e0} - \omega_{d0} \\ \varepsilon_{e0} \\ \varepsilon_{d0} \end{pmatrix} \right) = \begin{bmatrix} \omega'_{d0} \\ \omega'_{e0} \end{bmatrix}. \end{aligned} \tag{35}$$

Thus, the feed-forward compensation signal $\tilde{u}$ represents the angular velocities of the target at the point of linearization, which is as expected. The cross-coupling terms dependent on ω_r do not appear in the feed-forward compensation since they are state-related, and are therefore handled by LQ optimal regulator design that generates the signal $\bar{u}$.

4.6. LQ-Optimal Design. Steady-state LQ optimal design (Borrie, 1992; Kwakernaak and Sivan, 1972) is optimal in the sense that the regulator is designed to generate a control signal that minimizes a linear quadratic cost function V:

$$V = \int_{t_0}^{\infty} \left(x^T E x + u^T F u\right) \mathrm{d}t. \tag{36}$$

E is a positive semi-definite weight matrix that defines a quadratic function of the states that is to be minimized. F is a positive definite weight matrix that defines a quadratic function of the control inputs, and this term ensures that the control effort does not exceed physical limits. In this application, E and F are therefore set to represent the relative importance of regulating the angular error states ε_e and ε_d to zero while keeping the angular velocity set points ω_e and ω_d within acceptable limits.

Given the linear dynamic system in (33), the first step in regulator design is to solve the algebraic Ricatti equation for P:

$$0 = PA_0 + A_0^T P - PB_0 F^{-1} B_0^T P + E. \tag{37}$$

The control signal is then produced by the feedback of the states:

$$\bar{u} = -F^{-1} B_0^T P x, \tag{38}$$

where x represents now the state estimates produced by the local Kalman filter.

Substituting this back into (33) yields the closed loop dynamics:

$$\dot{x} = \left(A_0 - B_0 F^{-1} B_0^T P\right) x. \tag{39}$$

By design, this is guaranteed to be stable. Thus, feedback regulation of the states is achieved while minimizing the cost function V.

At each point of linearization, the process of regulator design must be repeated. The weight matrices E and F do not need to be changed for each redesign since the priorities of minimising the position error states while keeping the control signals low remain the same throughout.

Other possible regulator designs exist as well. One example is alternative LQ optimal design that regulates the states to zero by the end of a finite time period. The solution is a regulator with time-varying gains that are specified over the control time horizon. The specification of the end time is, however, an open problem, and the design makes no attempt to maintain the states at zero after the end time. In this tracking problem, the regulation of the errors is required over an undetermined period. Furthermore, finite-time horizon design requires prior knowledge of any parameters over the time period, which is impractical since disturbance inputs and target attributes are not known in advance.

Another possibility would be to use a predictive control strategy with a receding time horizon (Mayne *et. al*, 2000; Soeterboek, 1992). This would overcome the problem of specifying a particular end-time point. The reference trajectory for the position errors over the horizon would simply be zero. A receding time horizon design would also fit into the LQAdaptive framework easily since the repeated linearization process handles the effects of disturbances at each time instant and, therefore, lends itself naturally to an updating control law. However, solving the optimization problem is still computationally difficult, and this could have an impact on the frequency of linearization. Hence, the choice of steady-state LQ optimal control is a practical and realisable solution to regulator design.

4.7. Control Law. The overall control law is thus composed of the feed-forward compensation of the target velocities and the feedback regulation of the position errors:

$$\begin{aligned} u &= \tilde{u} + \bar{u} \\ \Rightarrow \begin{bmatrix} \omega_d \\ \omega_e \end{bmatrix} &= \begin{bmatrix} \omega'_{d0} \\ \omega'_{e0} \end{bmatrix} - F^{-1} B_0^T P x. \end{aligned} \tag{40}$$

This control law is maintained for the period during which the linear approximation of the dynamics is used. At the next point of linearization, a new compensation signal must be calculated and a new feedback regulator designed.

The generated control signal u represents angular velocity set points for the tracker pitch and yaw axes in the constructed r-e-d frame. As has already been shown, the pitch axis set point can be actuated directly by the elevation axis, but the yaw axis set point must first be converted into a training axis set point. The following conversion is used:

$$\dot{\theta} = -\mathrm{sgn}\left(\omega_d\right) \sqrt{\omega_d^2 \left(1 + \tan^2 \varphi\right)}, \tag{41}$$

where $\dot{\theta}$ is the training axis velocity set point, ω_d stands for the yaw axis velocity set point as calculated by controller, and φ denotes the elevation angle. The 'sgn' component ensures a consistent definition of positive angular velocities in the r-e-d frame and the training axis.

Once the velocity set points ω_e and $\dot{\theta}$ have been generated, the elevation and training axes must physically actuate them. As has already been shown, this is carried out by inner velocity loops that are designed to accommodate disturbances such as friction and wind torques. The assumption throughout this paper is that velocity controllers work perfectly, and thus velocity set points are achieved immediately.

In summary, the simple estimator-regulator structure is designed without acknowledging that the separation principle does not apply to non-linear dynamics. The proposed LQAdaptive structure attempts to take the non-linear dynamics of the LOS model and develop an estimator and regulator that conform as closely as possible to the separation principle over each period of local linearized dynamics. This should yield improved tracking performance over the simple estimator-regulator structure.

5. Simulation

A simulation was set up that modelled a target flying in a straight line past the tracker. The units for specifying the distances and speeds of the target in the standard x-y-z frame were arbitrary since only the resultant angular rates were important. Figure 7 shows the angular velocities in the LOS coordinate frame r'-e'-d' of the test profile.

Given the significant non-zero angular acceleration in the first 10 seconds of the profile, the first phase can be considered 'high manoeuvring'. This tests the ability of the control system to track a demanding target that forces high rates of acceleration in the elevation and training axes. The second phase is at near zero angular velocity and, therefore, it tests the tracker's ability to reject any disturbances while holding steady.

The inner velocity loops was not modelled in the simulation, so perfect and instant actuation of the velocity set

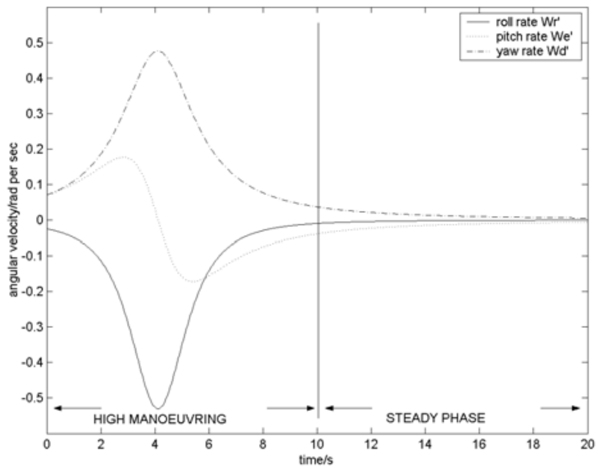

Fig. 7. Test profile angular rates.

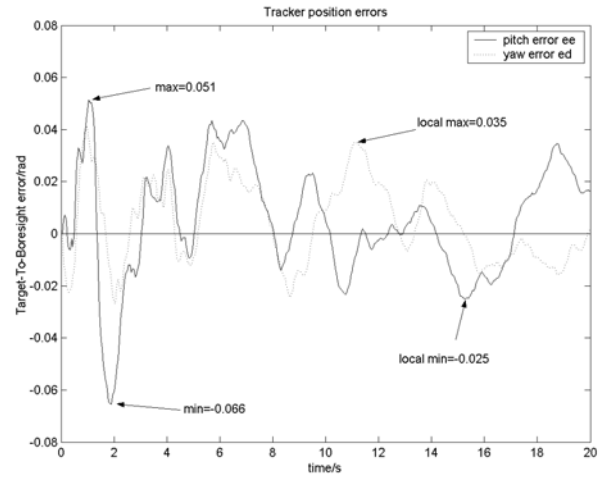

Fig. 8. Pitch and yaw errors under estimator-regulator control.

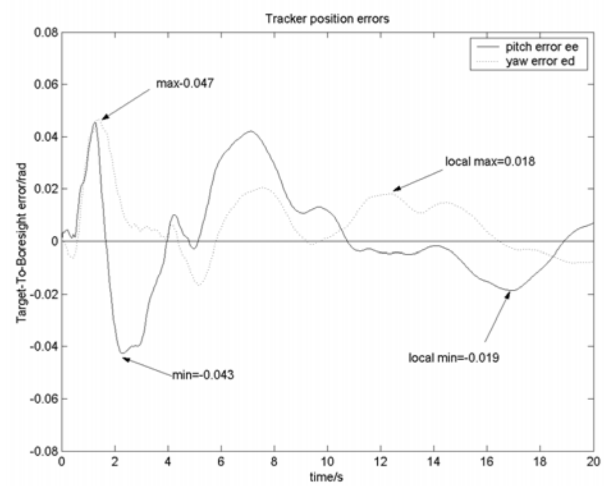

Fig. 9. Pitch and yaw errors under LQAdaptive control.

points was assumed. Work already carried out on velocity loop design proposes regulator gains of $k_p = 4$ and $k_i = 3$ that would be suitable for real implementation of the loops, so these gains were used in the simulation for the simple estimator. For the LQAdaptive controller, the weight matrices E and F were set such that the relative weights of the pitch error, yaw error, pitch velocity control signal and yaw velocity control signal were all equal. This was so that equal priority would be given for minimizing the position errors and keeping the control signals acceptably low.

Additive white Gaussian measurement noise was introduced to corrupt the simulated range, pitch error and yaw error readings. In reality, sensor noise is likely to be correlated with the target range, but this was not modelled for simplicity.

Good quality performance of the tracker was defined as a response that kept the absolute pitch and yaw errors as small as possible. This is because other systems on the ship may require the tracker to provide target information at any instant. Thus a small continuous error is preferable to perfect tracking that can suddenly be lost. The simulation was run first with the simple estimator-regulator structure as the control system, and then secondly with the LQAdaptive structure. The precise measurement noise and disturbance scenarios were the same in both runs. Figure 8 shows the resultant pitch and yaw errors under the simple control system, while Fig. 9 shows the same errors under the LQAdaptive system.

It can be seen that under LQAdaptive control, the performance was better for exactly the same test profile, since the peak errors in both the high manoeuvring and steady phases were smaller compared with the simple controller. In terms of absolute maximum errors in either axis, the largest under the simple controller is 0.066 rad, while under LQAdaptive control it is only 0.047 rad.

In addition to that, the error plots are considerably smoother under LQAdaptive control, showing that much smoother control of the axes was achieved. This would lead to less mechanical wear of the tracker. Also, in the steady phase of the target profile, the regulation of the errors due to the effects of disturbances and sensor noise is noticeably better with LQAdaptive control, unlike with the simple control, where large and frequent fluctuations in the errors are visible.

Although the general smooth response of the LQAdaptive controller was clear from Fig. 9, further testing was carried out to ensure that the absolute peak error was indeed reduced under LQAdaptive control. The simulation was repeated 300 times for both the simple controller and the LQAdaptive controller using the same test profile, but with a new measurement noise scenario for each repeat. The absolute peak errors in the pitch and yaw axes over the high manoeuvring phase were recorded for each controller, and the distributions of these errors are seen in Figs. 10 and 11.

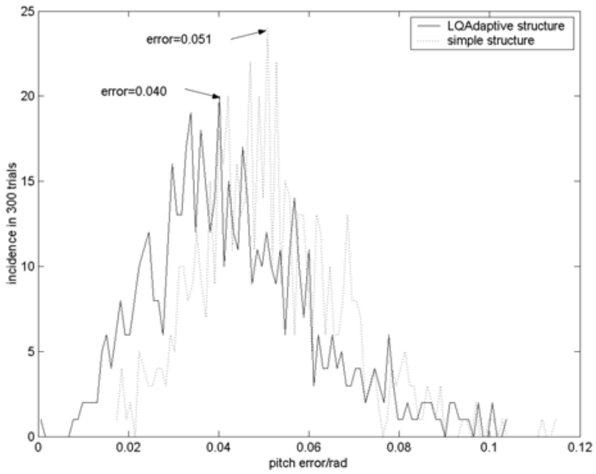

Fig. 10. Distribution of absolute maximum pitch errors.

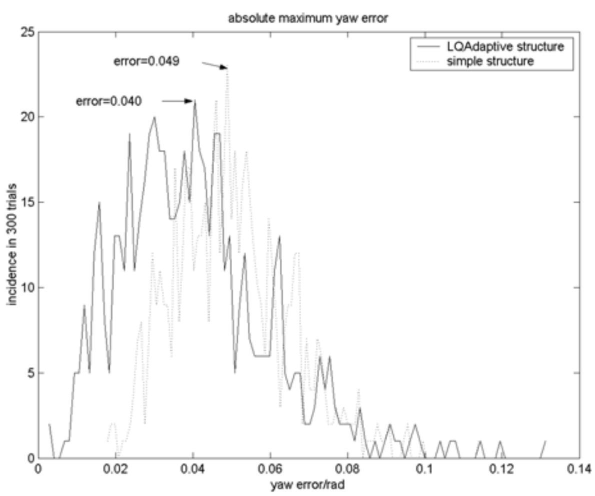

Fig. 11. Distribution of absolute maximum yaw errors.

In both cases, the centres of the distributions for the LQAdaptive responses are lower than those for the simple estimator-regulator responses. With the spreads being roughly equal, this suggests that the LQAdaptive controller manages to handle the measurement noise and disturbances better than the simple controller for the same test profile.

6. Conclusions

A ship-based two-axis target tracker was presented. The non-linear dynamic model of Line-Of-Sight (LOS) errors between the tracker and the target was detailed, and this was used to derive a regulator that drives the LOS errors to zero. The regulator includes a feed-forward component based on target angular velocities that cannot be measured. Estimation is thus required, and an extended continuous Kalman filter is introduced to provide the relevant velocities, along with filtered estimates of the input sensor data. Both the regulator and the Kalman filter are already available, and each component is known to function well individually. The problem addressed in this paper is how to integrate the two components together to form an overall closed loop position controller.

A simple control system is constructed by simply cascading the Kalman filter and the regulator together in a closed loop system. The performance of this system is likely to be suboptimal, since the separation principle does not hold in non-linear problems. A new control system labelled the ‘LQAdaptive structure’ is proposed that aims to improve conformity to the separation principle. This is done by introducing a local filter to ensure the compatibility of state spaces, and by using Linear-Quadratic optimal regulator design on local linearized dynamics. As a result, over each short period of local linear dynamics, a near optimal Kalman filter is cascaded with an optimal regulator in the closed loop system.

Simulations were carried out to compare the responses of the two position control systems to a test target profile. Perfect tracker axis actuation was assumed. The results showed that control under LQAdaptive structure was considerably smoother than under the simple structure. Repeated trials with random measurement noises also showed that the peak errors that occur during tracking are generally smaller under LQAdaptive control than under the simple controller.

In summary, the attempt to improve conformity to the separation principle led to a control system that achieves better tracking under the simulation assumptions. Further testing would be required to incorporate the true axis dynamics and velocity controllers in order to get a more realistic view of the tracker responses.

It was also assumed that the elevation angle φ is available directly as a measurement, which may not be the case in reality. Acquiring a value of φ may present its own technical challenges, but the incorporation of the value into the LQAdaptive structure should still yield the same results. One available option is to relate the angle to the known dynamics and carry out extended estimation. It can also be seen that any improvement in tracking is traded against the increased complexity of the LQAdaptive control system. The implementation of a rapidly adapting control law may pose problems in the reliability and robustness of any hardware and software used.

References

Borrie J.A. (1992): *Stochastic Systems for Engineers: Modelling, Estimation and Control*. — New York: Prentice-Hall.

Brdyś M.A. and Littler J.J. (2002): *Fuzzy logic gain scheduling for non-linear servo tracking*. — Int. J. Appl. Math. Comput. Sci., Vol. 12, No. 2, pp. 209–219.

Ekstrand B. (2001): *Tracking filters and models for seeker applications*. — IEEE Trans. Aerosp. Electron. Syst., Vol. 37, No. 3, pp. 965–977.

Jaźwiński A.H. (1970): *Stochastic Processes and Filtering Theory*. — New York: Academic Press.

Kwakernaak H. and Sivan R. (1972): *Linear Optimal Control Systems*. — New York: Wiley.

Mayne D., Rawlings J.B., Rao C.V. and Scokaret P.O.M. (2000): *Constrained model predictive control: Stability and optimality*. — Automatica, Vol. 36, No. 6, pp. 789–814.

Singer R.A. (1970): *Estimating optimal tracking filter performance for manned maneuvring targets*. — IEEE Trans. Aerosp. Electron. Syst., Vol. 6, No. 2, pp. 473–483.

Soeterboek R. (1992): *Predictive Control – A Unified Approach*. — Hemel Hempstead: Prentice–Hall International.

Yang Z. (2002): *Multiple-model tracking with fixed-lag smooting using imprecise information*. — Ph.D. thesis, Department of Electronic, Electrical and Computer Engineering, The University of Birmingham, Birmingham.

Received: 13 October 2005
Revised: 22 January 2006